



International Journal of Current Research and Academic Review

ISSN: 2347-3215 Volume 3 Number 4 (April-2015) pp. 74-88

www.ijcrar.com



Determination of optimal heat treatment temperature for the fabrication of Ag/TiO₂ composite thin films using Molecular Precursor Method (MPM)

Daniel S. Likiusa* and Uahengo Veikkoa

Department of Chemistry and Biochemistry, Faculty of Science, University of Namibia
340 MandumeNdemufayo Avenue, Private bag 13301, Windhoek, Namibia

*Corresponding author

KEYWORDS

Titania,
Heat-treatment
temperature,
Molecular
Precursor
method,
Anatase,
Rutile

A B S T R A C T

This article presents a study on the effect of heat treatment temperature on the crystalline anatase to rutile phase transformation of silver nanoparticles /titanium dioxide (Ag-NP/TiO₂) composite thin films, successfully synthesised by molecular precursor method (MPM). Respective precursor solutions for Ag-nanoparticles and titania were prepared from Ag salt and a titanium complex, spin-coated on quartz glass substrates and heat treated at different temperature, namely; 250, 300, 400, 500, 600, 700 and 800°C. The effect of employing various heat treatment temperatures on phase transition is systematically studied by XRD, XPS, EDX, SEM and TG/DTA curve. X-ray diffraction (XRD) pattern peaks revealed that the temperature of calcination is critical in determining the crystallinity of the TiO₂ and silver nanoparticles (Ag-NPs). For pure TiO₂ as expected, anatase was transformed to 100% rutile at 600°C. However, doping of a titanium precursor with a silver precursor solution results in extended transformation temperature. At 700°C, Ag-NP/TiO₂ composite thin films samples consist of both anatase (45%) and rutile (55%). XPS results shows that the low mechanical energy associated with the silver oxide formation during the cool down of metallic silver in Ag/TiO₂ composite thin films heat-treated at temperature between 600—700°C decelerated the phase transformation of anatase to rutile. Mixed-phase photocatalysts with rutile–anatase compositions have been reported to exhibit enhanced photoactivity relative to single-phase titania.

Introduction

Specific heat treatment temperature causes the changes in material structure, nature of distribution of the nanoparticles/crystallites in the film, material density, desorption of volatile impurities from the film surface

depending on the method, dopants, temperature, time etc (Ma *et al.*, 2010). The effects of heat treatment temperature are expected to be reflected in the crystal phase of the films. TiO₂, which is generally used in

photocatalytic air and water purification and many other purposes based on photocatalytic oxidation and decomposition of organic pollutants, is a material of great interest. TiO_2 has three crystal phases: anatase (tetragonal), rutile (tetragonal) and brookite (orthorhombic). Among them, the anatase is a meta-stable phase and has a band gap (3.2 eV) higher than the other ones. In the synthesis of TiO_2 films by various methods, the initial crystalline TiO_2 phase formed is generally anatase. However, anatase phase may be transformed to rutile phase with heat treatment (Stamate *et al.*, 2008). The rutile structure has a band gap of 3.0 eV and is the most common white pigment in paint products due to its extremely high refractive index ($n = 2.8$) (Toda *et al.*, 2003). It should be noted that it is possible to form rutile under near room temperature conditions (Shin *et al.*, 2005; Li *et al.*, 2004). Hydrothermal methods of synthesis, which can facilitate the precipitation of crystalline TiO_2 directly from a liquid phase, can be controlled to precipitate rutile. Aside from this method, rutile is obtained through high-temperature treatment. Brookite is difficult to synthesize and so is seldom studied (Landmann *et al.*, 2012).

The production of high photoactivity material with high temperature anatase phase stability is one of the key challenges in smart coating technology nowadays. Increase in temperature allows the structural transformation of TiO_2 from anatase to rutile irreversibly at elevated temperatures (Shchipunov and Postnova, 2009). It is well known that temperatures that promote the anatase to rutile transformation, which can take place anywhere between 400 and 1,000 °C, depending on the coating solution characteristics (Kim *et al.*, 2002; Hou *et al.*, 2003; Yu *et al.*, 2003). Recently, Behforooz *et al.*, (2012) review the differences between

the two main polymorphs of titanium dioxide, the nature of the anatase to rutile transformation, and the principles of controlling phase composition through the inhibition or promotion of the transformation of anatase to rutile. The temperature difference between the phase transformation from anatase to rutile in the sol-gel method and the MPM are reported by Nagai *et al.* (2008). Using conventional sol-gel method, the anatase phase appears during the heat-treatment of both precursor films at a temperature between 400 and 500°C (Nagai and Sato, 2012). By using MPM, anatase can be transformed to the rutile one between 500 and 700°C (Nagai *et al.*, 2008), while a sol-gel process reported by other authors (Czanderna *et al.*, 1958; Kumar *et al.*, 2000; Yoganarasimhan and Rao, 1962; Uekawa *et al.*, 2003) showed that anatase could not transformed to the rutile one, even when heat-treated at 900°C.

Although numerous techniques have been applied, the majority of these efforts are through doping of the TiO_2 with; noble metals, transition metal ions, or anions (Reddy *et al.*, 2011; Tian-hua *et al.*, 2006; Akpan and Hameed, 2010; Meng *et al.*, 2012; Guana *et al.*, 2013). Of particular interest in this paper is the doping of TiO_2 with silver to form Ag/TiO_2 . In term of doping titania with silver as a foreign agent, it has been shown that the introduction of Ag, even in small amounts, can greatly affect TiO_2 -based thin film properties including; crystallinity, morphology, and chemistry (Akgun *et al.*, 2011). Various processing parameters, including heat treatment temperature and time can be used to control phases transformation of titania in Ag/TiO_2 thin films (Stamate *et al.*, 2008; Behforooz *et al.*, 2012; Akgun *et al.*, 2011; Azizi and Bagheri-Mohagheghi, 2013). The kinetics of these processes typically is considered in this paper in terms of

temperature while keeping heat treatment time and the atmospheric environment constant.

In this research, the MPM will be employed. The MPM has many advantages with respect to the other fabrication techniques in terms of crystallinity, purity, homogeneity and stability. Moreover, using MPM, the metal complex ions dissolve independently in each precursor solution and the homogeneity of the mixed solution can be kept at the molecular level (Nagai and Sato, 2012). On the basis of this excellent miscibility in the MPM, two precursor solutions of titania and silver with a 1:1 mixed molar ratio was used to fabricate Ag-NP/TiO₂ composite thin films and heat treated at different temperatures. The structural and morphological properties of silver/titania nanoparticles were studied using X-ray diffraction (XRD), X-ray photoelectron spectroscopy (XPS), field-emission scanning electron microscope (FE-SEM) and thermal gravimetry/differential thermal analysis (TG/DTA). Mixed-phase photocatalysts with rutile–anatase compositions have been reported to exhibit enhanced photoactivity relative to single-phase titania (Czanderna *et al.*, 1958; Kumar *et al.*, 2000; Yoganarasimhan and Rao, 1962). The aim of this paper is to find the optimal heat treatment temperature that will allow a researcher to fabricate pure, homogeneous, stable, and 1:1 mixed-phase Ag-NP/TiO₂ composite thin films with rutile–anatase compositions. The advantages of obtain a 1:1 mixed-phase of anatase-rutile rather than anatase and rutile separately is that: anatase is not stable enough to exist alone and rutile is photo inactive to act as a photocatalyst.

Experimental procedures

Materials

Silver acetate and dibutylamine were

purchased from Wako Pure Chemical industries, Ltd. Ethylenediamine-N,N,N',N'-tetraacetic acid (EDTA) and titanium tetraisopropoxide (Ti(OⁱPr)₄) were purchase from Kanto Chemical Co., Inc. 30% H₂O₂ were purchased from Santoku Chemical Industries Co., Ltd., respectively. Methanol and 2-propanol were purchased from Taisei Chemical Co., Ltd. while ethanol was purchased from Ueno Chemical Industries, Ltd and dried on 4A molecular sieves prior to use. Other materials were used without further purification. Silver plates used as counter electrode was purchased from NISSHIN EM Co.

Polished quartz glasses were purchased from Akishima Glass Co., Ltd. The glass substrates of 20 × 20 × 1.1 mm³ were prepared and cleaned in 2-propanol with an ultrasonic bath to remove physisorbed organic molecules from the surfaces, followed by rinsing several times with de-ionized water. Then the substrates were dried in a drying oven at 70°C.

Fabrication procedures of a thin film

Substrate cleaning process

High quality thin films require ultra clean glass substrate surface without particle contamination, metal contamination, organic contamination, ionic contamination, water absorption, native oxide and atomic scale roughness. It's considered that this substrate cleaning process is very important to realize the fabrication of a desirable thin film that can undergo reproducibility.

Herein, the quartz glass substrates that are used as supportive surfaces for the thin films were cleaned on a basis of cleaning process, which was proposed in our laboratory. The first step, which use a solution of surfactant/alkaline as detergent/water (H₂O)

(detergent : H₂O = 5 : 95), was performed to remove any organic material and metallic impurities.

This was followed by rinsing the glass substrates several times with DI water. After that, these glass substrates were cleaned with 2-propanol (IPA) in an ultrasonic bath to remove physisorbed organic molecules, natives and chemical oxides from the surfaces. Quartz glass substrates with dimensions of 20×20×1.5 mm³ were ultrasonically cleaned in 2-propanol for 20 min and then the wafers were dried in a drying oven at 70°C.

Fabrication process of Ag/TiO₂ composite thin films by coating and heat treatment

The precursor solution containing a Ti⁴⁺ complex of EDTA, S_{TiO₂} was prepared in accordance with the MPM reported by current author and co-workers (Nagai and Sato, 2012; Nishide *et al.*, 2000). The Ag acetate ethanol solution S_{Ag} for the preparation of Ag-nanoparticle fabrication in the composite thin films was prepared according to the method we reported recently (Daniel *et al.*, 2012). The S_{TiO₂} and S_{Ag} solutions were then mixed at 1:1 molar concentration to form composite solution, S_{composite} as a thin film coating precursor solution. The S_{composite} were deposited by spin coating onto the cleaned quartz glass substrates with a double step mode: first at 500 rpm–5 s and then at 2000 rpm–30 s in all the cases. The resultant composite thin films were fabricated by heat-treatment at different temperatures (250–800°C) for 0.5h. Thin films of pure TiO₂ were also fabricated for comparison purpose by heat treating the spin-coated S_{Ti} precursor films at different temperatures. The photographs of seven Ag-NP/TiO₂ composite (Ag/TiO₂)_n thin films fabricated are shown in Figure 1. The number *n* in the notation of the

composite thin films indicates the heat treatment temperature for a given sample; for example, Ag/TiO₂700 indicates that the composite thin film was heat treated at 700 °C. Thin films of pure TiO₂ were also fabricated for comparison purpose by heat treating the spin-coated S_{Ti} precursor films at different temperatures.

Crystal structure, chemical composition and observation of surface morphology

Crystal structural, elemental composition and surface morphology of the fabricated thin films were performed using X-ray diffraction (XRD), X-ray photoelectron spectroscopy (XPS) and field-emission scanning electron microscope (FE-SEM), respectively. The (XRD) patterns of Ag particles, titania, and COMP-Agn films were measured using an X-ray diffractometer (MXP-18AHF22, BrukerAXS) with Cu–Kα rays generated at 45 kV and 300 mA. Parallel beam optics were employed with an incident angle of 0.3°. The anatase to rutile ratio, *f*, for titania and the COMP-Agn films was calculated with the empirical Eq. 1, using the peak ratio *I*/*I*₀: rutile (1 1 0) and *I*/*I*₀: anatase (1 0 1), according to the literature (Spurr and Myers, 1957). A XPS Phi Quantum 2000 Scanning ESCA Microprobe (Shimadzu) with a focused monochromatic Al-Kα X-ray (1486.6 eV) source was employed in order to evaluate the elemental states and quantities—Ti, O, C and Ag—in the thin films.

$$f = \frac{1}{1 + 1.26 \left(\frac{(I/I_0)_{rutile}}{(I/I_0)_{anatase}} \right)} \quad (1)$$

No critical surface charging during the XPS measurements was observed; thereby, no correction of binding energy was performed. The depth profiles were obtained with the identical instrument. The stepwise etching

was performed by bombarding the Ar⁺ ions with 2 kV for 3 min before measuring each layer. The surface morphology of the resultant films was observed using a FE-SEM (S-4200, Hitachi) at an accelerating voltage of 5.0 kV.

Crystallization behavior of a precursor solution under thermal condition

TG-DTA machine, (Model TAS-100, Rigaku, Japan) was employed. One thermocouple was placed in an Al₂O₃, while the other is placed in a sample of the *S_{composite}*.

Result and Discussion

Crystal structure of the thin films

Figure 2 shows the XRD patterns for pure TiO₂ films and Ag/TiO₂ composite thin films heat treated at different temperatures. The peaks found at $2\theta = 27.5, 36.2, 39.3, 41.4, 44.3, 54.5, 56.7, 64.2,$ and 69.2° , corresponding to the (110), (101), (200), (111), (210), (211), (220), (310), and (301) phases of rutile [JCPDS card 21-1276]. The peaks observed at $2\theta = 25.6, 38.1, 48.4, 54.2, 55.5, 62.9, 69.1, 70.7,$ and 75.3° , corresponding to the (101), (004), (200), (105), (211), (204), (116), (220), and (215) phases of anatase [JCPDS card 21-1272]. The peaks at $38.18, 44.39, 64.58,$ and 77.54° are assigned as the (111), (200), (220), and (311) reflection lines of fcc Ag particles (JCPDS file, No. 04-0783), respectively. Weak and broadened peaks in the spectra might be due to the small grains of the composites.

Pure TiO₂ thin films heat treated at 300°C and below are amorphous. At 400–800 °C the pure TiO₂ thin films have crystal phases. For Ag/TiO₂ composite thin film sample heat treatment at 400°C and below, no

diffraction peaks at 25.4° corresponding to titania were observed, indicating that TiO₂ was amorphous or well dispersed inside the silver/organic matrix, with a crystal size smaller than those of silver particles (Maldonado-Ho´dar *et al.*, 2000).

The intensity of the (111) and (200) diffraction peaks of Ag phases in figure 2, found to be increased as the heat treatment temperature is increasing up to 500°C. Sharp diffraction peaks indicated the formation of pure silver of high crystalline (Zhang and Oh, 2010). On the basis of the XRD results in Figure 2, and Eqs. 1, the anatase/rutile ratio (*f*) in the composite thin films, were calculated and tabulated in Table 1.

The decreasing trend of the *f* value clearly shows that the rutile content increases at the expense of anatase as heat treatment temperature increases. After heat treatment temperature above 700°C for 0.5 h, the peak intensity of anatase greatly decreased and the samples mainly consisted of rutile.

Usually, anatase transforms to rutile at high temperature such as 700°C in air from Ti-EDTA complex solutions (Grabowska *et al.*, 2013). This is exactly what happens for our pure TiO₂ thin film as illustrated in figure 2. However in the case of the Ag/TiO₂ composite thin films, 100% rutile phase could be only obtained at round 800°C. No extraneous peaks appeared under the heat treatment, only peaks for Ag metallic and TiO₂ were detected with the exception of the peak observed at 36.5° in the XRD pattern of the composite thin films fabricated at high temperature (600, 700 and 800°C); indicates the presence of silver oxide [JCPDS card 40-909]. Thermodynamics studies have suggested that silver is more stable than Ag₂O/AgO at temperature of $> 189.8^\circ\text{C}$ in air (Nishide *et al.*, 2000). Therefore, any of Ag₂O/AgO that is present decomposed to metallic silver during heat treatment stage.

The small amount of Ag₂O that appear in the XRD may be formed during the cooling stage. These results indicated that low mechanical energy associated with silver oxide decelerated the phase transformation of anatase to rutile, thus delay the transformation of anatase to 100 % rutile until round 800°C.

Chemical composition of the Ag/TiO₂ composite thin films

We performed depth profiling XPS to further clarify changes in chemical states and electronic structures with change in heat treatment temperature. Figure 3 shows the XPS high resolution wide scans for Ag/TiO₂ composite thin film heat treated at 600°C. The major XPS peaks include C1s Ag 3d, Ti 2p and O1s (Figure 3 insets). The carbon might come from two sources: adventitious element carbon from the impurity of equipment chamber, and carbon residues from the impregnation of alcoholic precursor.

For narrow scan, the depth profile for Ag/TiO₂ composite thin films at different heat treatment temperatures were also performed and are tabulated in Table 2. The high resolution Ag 3d peaks for all thin films are located at 370.6 eV (3d_{5/2}) and 376.7 eV (3d_{3/2}) on average. The interpretation of Ag 3d peaks is rather delicate because the chemical shifts between metallic and oxide phases are very weak. However, it is now admitted that oxide contributions generate negative shift (Grabowska *et al.*, 2013).

The shift is usually smaller for Ag₂O (0.3–0.4 eV) and larger for AgO (0.8–1.0 eV) (Han *et al.*, 2012). The best way to evaluate this is to consider the spin-orbital splitting. The metallic Ag is known to exhibit a spin–orbit splitting of 6.0 eV (Kang and Sohn, 2011). All the Ag/TiO₂

composite thin films exhibit such spin-orbital splitting of 6.0 eV, hence this is attributed to mainly metallic Ag (Kang and Sohn, 2011; Zhang *et al.*, 2000), consistent with the XRD result reported above.

The Ti 2p_{3/2} peak (Table 3) is found in the range of 458.1–459.69 eV (within experimental uncertainty), attributed to Ti⁴⁺ for pure crystalline TiO₂ (Han *et al.*, 2012; Huang *et al.*, 2012). The Ti 2p_{3/2} binding energy band at lower heat treatment temperature (70 to 400°C) shifts to a higher position than those fabricated at higher heat treated temperature (500–800°C), indicating a decrease in electron density of the Ti atoms in the Ag/TiO₂ composite thin film samples with increase in the heat treatment temperature.

Spectral changes in the O1s region of XPS spectra provided more quantitative information on the kinetics of Ag oxide and TiO₂ formation. Peak values of high-resolution spectra of O1s obtained from the samples heat treated at different temperature are presented in Table 3. The O1s spectra are broad and complex (Fig. 3, insets), suggesting contributions of several oxygen species. A peak at 530.6 eV is attributed to Ag₂CO₃ and adsorbed CO₂ (530.5–531.0 eV) (Kang and Sohn, 2011).

A broad peak at 531.9–532.0 eV is associated with dissolved oxygen (530.5–531.5 eV) (Huang *et al.*, 2012). Therefore, the O 1s peaks (Fig. 3) found at 530.9–537.9 eV wide range region is decomposed into several contributions.

The main contribution is attributed to Ti-O in TiO₂ (Nasser, 2000). The other kinds of oxygen contributions can be counted by Ti-O bond of hydroxyl groups from alcohol precursor, the C-O bonds and the adsorbed H₂O, respectively

TG/DTA of the Ag/TiO₂ composite thin films

The presence of unintentional impurities or intentional dopants has a strong effect on the kinetics of the anatase to rutile transition (Hanaor and Sorrell, 2011). TG-DTA peak apices can be considered to be applicable for comparative analysis of the phase transformation considering the impurities. TG/DTA analysis shown in figure 4 indicates that residual organic substances have exotherm maximum at 343.2°C and then at 463.7°C and completely burned out at about 513.4°C. Therefore all the prepared samples heat treated at around 463.7°C will result in the transformation of titania amorphous to crystalline anatase phase. However, high crystalline anatase is only expected to be formed at around 513.4°C when complete combustion took place thus a very sharp exothermic peak is observed due to the formation of anatase phase. During heat-treatment of anatase, the atoms in the original tetragonal lattice can be rearranged into the rutile tetragonal lattice.

From these results, DTA analysis results seem to yields higher transformation temperatures than XRD analysis. This probably is a result of the sigmoidal form of the kinetics curve, as shown subsequently. That is, the phase transformation commences slowly at an onset temperature of 463.7°C and so it is more likely that the exothermal maximum (viz., the apex) is observed later in the phase transformation process, when the transformation rate is greatest; the rate of transformation subsequently decreases along with the corresponding latent heat as anatase converts to rutile. Usually, heat treatment at 450°C afforded an anatase phase, while treatment at 700 °C yielded a 100% rutile phase using sol-gel method (Ji *et al.*, 2012). Hu *et al.* (2003) have reported that TiO₂

normally undergone an anatase-to-rutile phase transition at around 600–700°C. While using MPM, Nishide *et al.* (2000) reported that anatase appeared in the gel at firing temperatures between 450 and 500°C, and was only transformed to rutile at temperatures between 550 and 600°C.

For thermal gravimetry analysis, a TG curve in Figure 4, can be divided into three stages. The first stage is from room temperature to around 285°C. The rate of weight loss is the greatest, up to approximately 53%, which is caused by dehydration and evaporation of alcohol contained in the composite precursor. The second stage is from 285 to 513°C. The rate of weight loss is approximately 34%, which is assigned to the combustion and carbonization of organic materials. However, some carbon element still exists in the films, which can be seen from the results of XPS studies above. The third stage is from 513 to 1000°C. The rate of weight loss is approximately 7%, which is attributed to oxidation of residue carbon and evaporation of chemisorbed water. Apart from the oxidation of residue carbon, the mass of the material did not change, reflecting that the polymorphs associated with titanium dioxide are the only one that are changing their phases.

FESEM images of the Ag/TiO₂ composite thin films heat treated at different temperatures

The effects of heat treatment are expected to be reflected on the surface morphology of the films. To study the dependence of the surface morphology of the Ag/TiO₂ composite thin films upon heat treated at different temperature, the FE-SEM images were taken for the Ag/TiO₂ composite thin films heat treated at different temperatures and such FE-SEM images are shown in figure 5. White dots represent Ag grains confirmed by EDX mapping shown in figure

6 below whereby the large particles on the surface elucidated that these particles correspond to the Ag element. Thus, the presence and distribution of Ag particles on the surface of the Ag-NP/TiO₂ composite films can be also reflected and observed in the FE-SEM images. The dense structures of silver nanoparticles seem to be increasing with the increase in heat treatment temperature.

The SEM image of films annealed at 300°C and 400°C has a lower contrast compared to that of films annealed at higher temperature, indicating the possible presence of organic block coverage on the films. Their surface is relatively smooth, and very few pores are observed. Thin films heat treated at higher temperatures had a highly porous network structure, with continuous porosity. This tells us that heat treatment temperature changed the morphology characteristics and structure of the thin films, allowing the thin films to develop higher porosity with increase temperature.

Table.1 The titania phases and anatase/rutile ratio, f of the Ag/TiO₂ composite thin films fabricated on a quartz glass using the mixed precursor solution Scomposite

Heat treatment temperature (°C)	Phases of Pure TiO ₂	Phases of Ag/TiO ₂
Ag/TiO ₂ 250	Amorphous	Amorphous
Ag/TiO ₂ 300	Amorphous.	Amorphous
Ag/TiO ₂ 400	Anatase only	Amorphous
Ag/TiO ₂ 500	Anatase only	Anatase only
Ag/TiO ₂ 600	Rutile only	Anatase-rutile (0.53:0.47)
Ag/TiO ₂ 700	Rutile only	Anatase-rutile (0.45: 0.55)
Ag/TiO ₂ 800	Rutile only	Rutile only

Table.2 XPS peak value for Ag/TiO₂ composite thin films at different heat treatment temperatures

Heat treatment temperature (°C)	Ag3d _{5/2}	Ag3d _{3/2}	Ti2p _{3/2}	O1s
Ag/TiO ₂ 250	372.3	378.2	459.3	537.9
Ag/TiO ₂ 300	372.4	378.3	459.1	535.3
Ag/TiO ₂ 400	372.0	378.2	459.6	534.6
Ag/TiO ₂ 500	368.1	374.3	458.1	531.1
Ag/TiO ₂ 600	367.8	373.9	458.5	530.9
Ag/TiO ₂ 700	370.1	376.4	458.7	533.0
Ag/TiO ₂ 800	369.3	375.8	459.8	532.5

Fig.1 Photographs a–h, of the Ag-NP/TiO₂ composite thin films fabricated by heat-treatment at different temperatures: a 250, b 300, c 400, d 500, e 600, f 700, and g 800°C, respectively for 0.5h in air

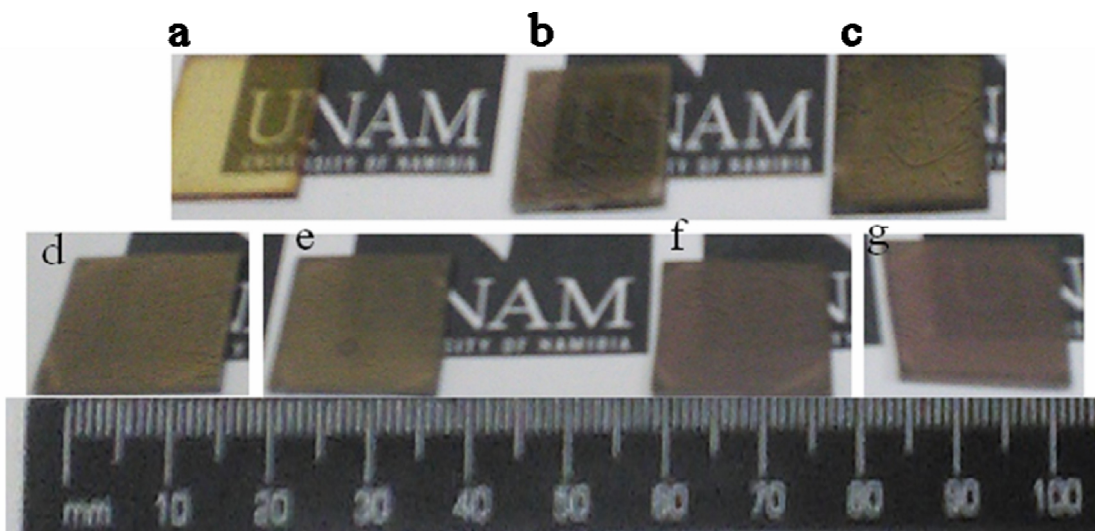


Fig.2 XRD of (a) Pure TiO₂, (b) Ag/TiO₂ composite thin films heat treated at different temperatures fabricated by MPM. The peaks of each phase are denoted as follows: filled inverted triangle silver, filled circle anatase, and filled square rutile

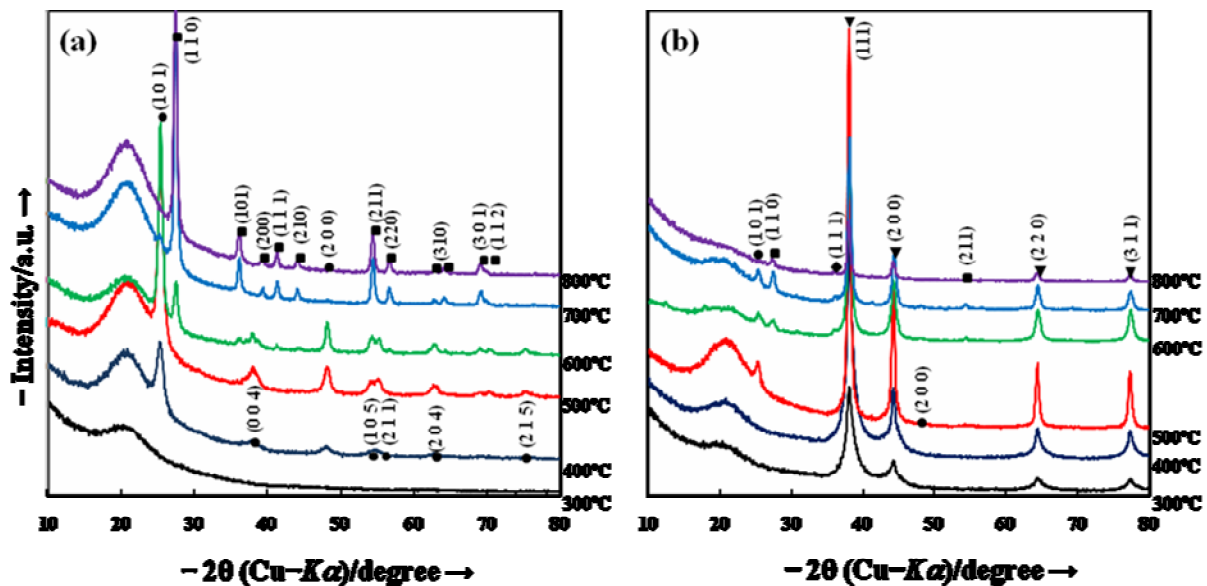


Fig.3 Representative wide-scan XPS survey spectrum taken from the surface of Ag/TiO₂ composite thin films heat treated at 600°C

Fig.4 TG/DTA curves of Ag/TiO₂ composite precursor solution (Scomposite)

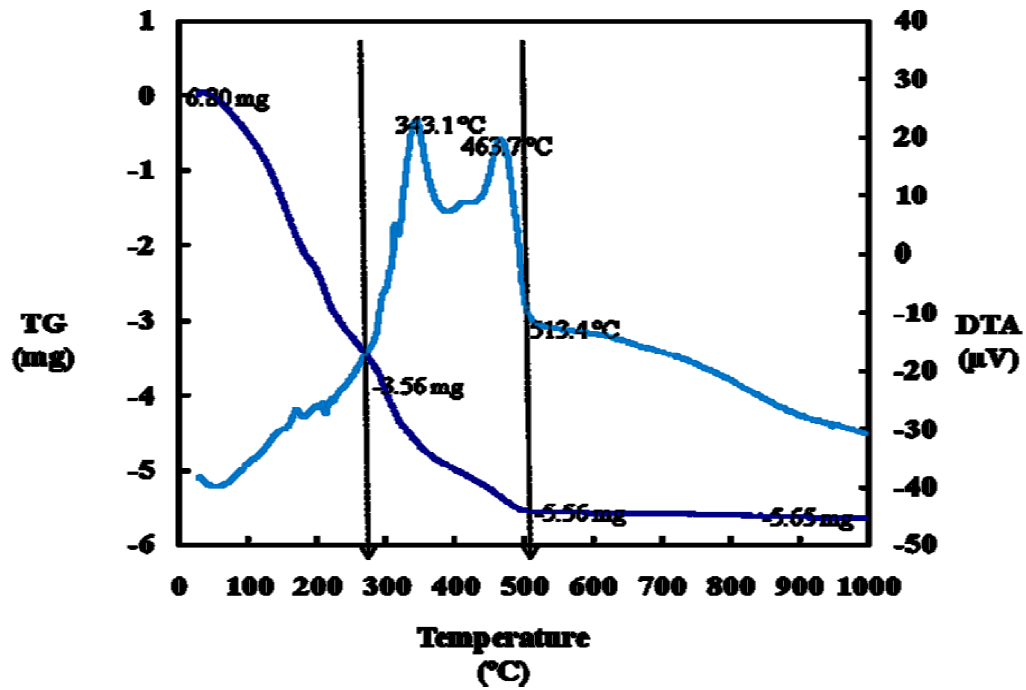


Fig.5 FE-SEM images of the Ag-NP/TiO₂ composite thin films (a-f) fabricated at different heat treatment temperature of 300, 400, 500, 600, 700, and 800°C respectively

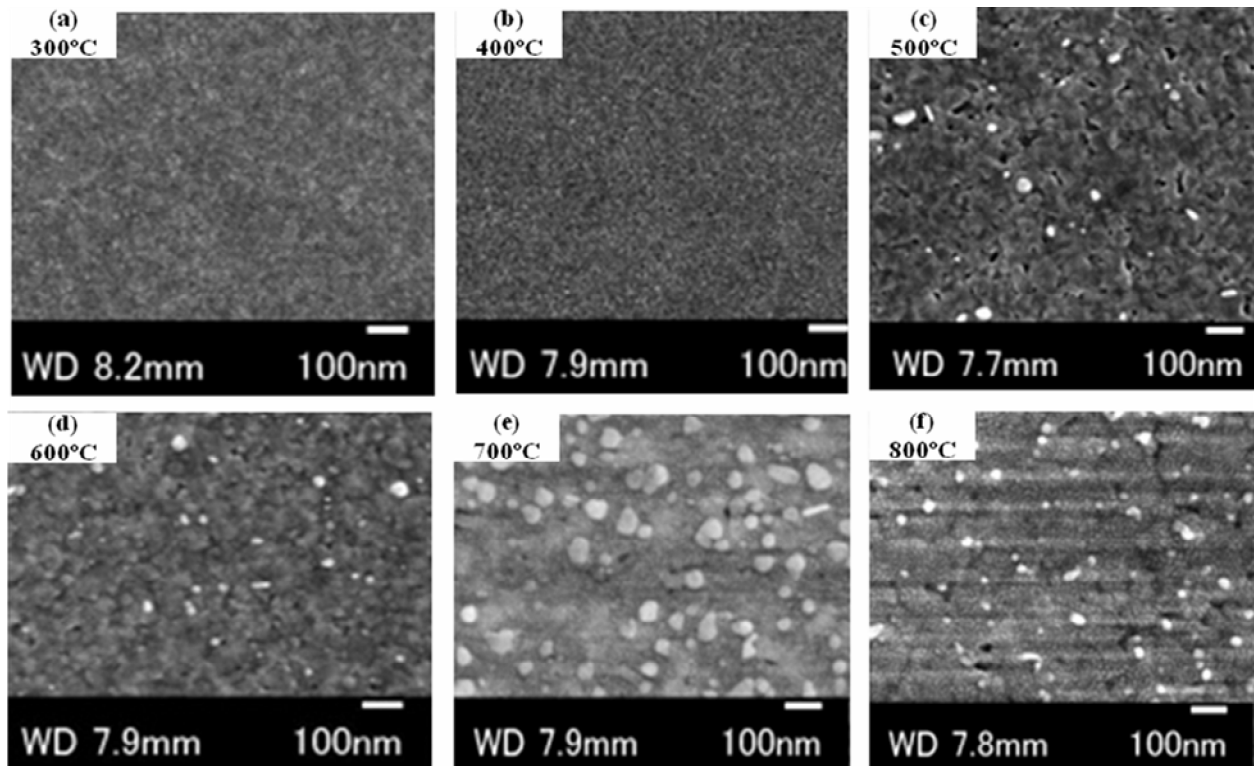
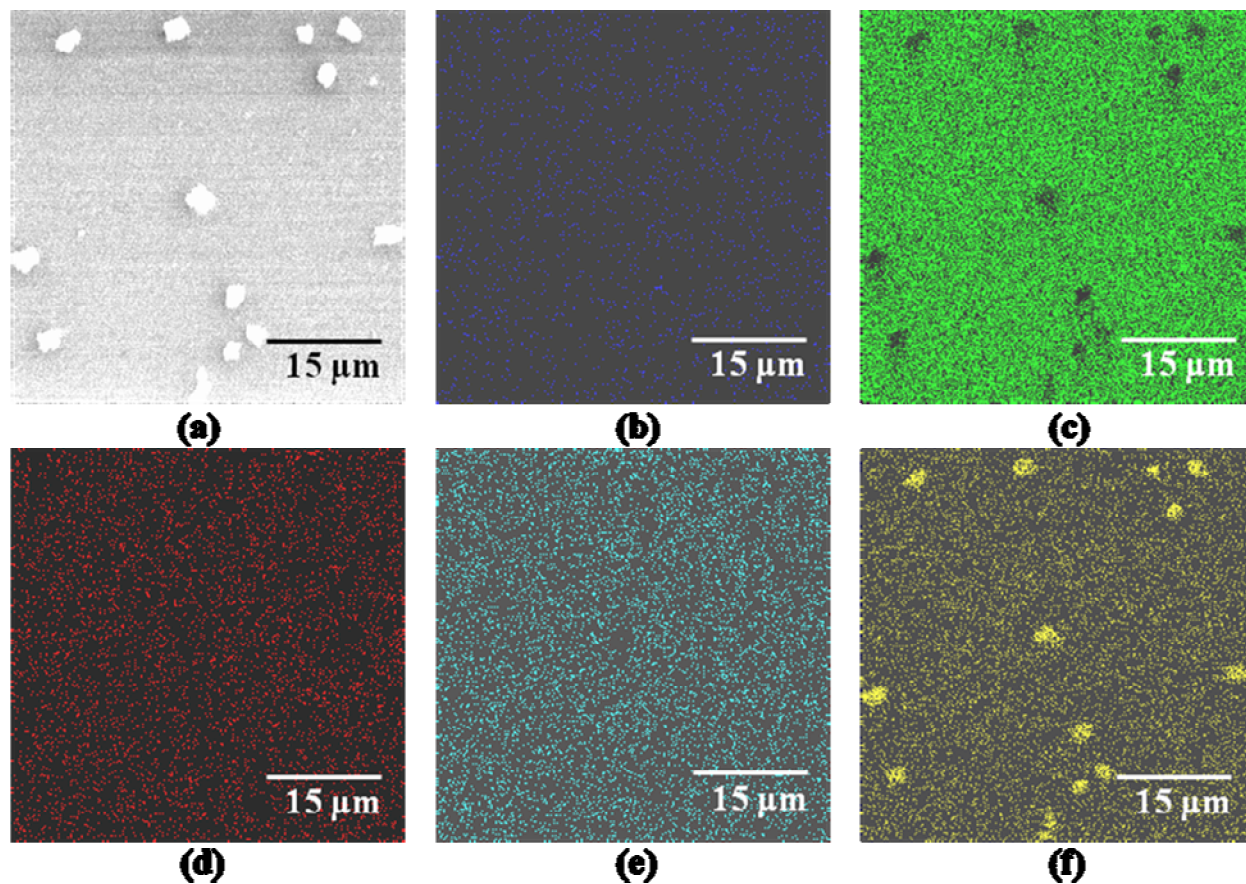


Fig.6 Elemental mapping of Ag/TiO₂ composite thin films fabricated at 600 C, observed by using energy-dispersive X-ray spectroscopy at an accelerating voltage of 20 kV. (a), (b), (c), (d), (e), and (f) were indicated surface appearance, C K α , Si K α , Ti K α , Ti L α 1, and Ag L α 1 map, respectively



Moreover, the Ag nanoparticles are being increasing on the surface of the thin film with increase of heat treatment temperature. The lack of agglomerated Ag NPs on the surface of the thin film for lower temperature thin films could be that the Ag particles are too small, hence are trapped inside the organic structure of the incomplete combustion of $S_{\text{composite}}$ (Spurr and Myers, 1957). At the highest heat treatment temperature (800°C), the surface became cracked and irregular (Figure 4f), which was in agreement with the results reported by Ishizawa and Ogino (1999).

Conclusion

In this paper, the Ag/TiO₂ composite thin films were synthesized by MPM and the effects of different heat treatment temperatures on transition of the anatase phase to rutile phase in air have been investigated. An understanding of the transformation of anatase to rutile is of great importance to those studying TiO₂ for photovoltaic, photocatalyst and other applications. The phase composition of the material has significant consequences on its properties and performance and therefore it

may be desirable to enhance or inhibit the transformation to give a particular phase or phase mixture subsequent to thermal treatment. Low mechanical energy associated with the silver oxide observed in XPS during the cool down of metallic silver in Ag/TiO₂ composite thin films heat-treated at temperature at 600–700°C decelerated the phase transformation of anatase to rutile. This deceleration results in the fabrication of 45:55 mixed phases of anatase: rutile ratio at 700°C. Therefore, 700°C is an optimal temperature for obtaining a mixed-phase with anatase-rutile with appropriate composition that deserves a further investigation of photocatalytic and photovoltaic studies.

Acknowledgments

This study was supported by the office of the Vice Chancellor of the University of Namibia (UNAM) and UNAM Foundation. Matching fund subsidy from MEXT (Ministry of Education, Culture, Sports, Science and Technology), Japan. Most experiments were carried out in the Coordination Chemistry laboratory, Kogakuin University, Tokyo, Japan.

References

Akgun, B.A., Durucan, C., Mellott, P.N. 2011. Effect of silver incorporation on crystallization and microstructural properties of sol–gel derived titania thin films on glass. *J. Sol-Gel. Sci. Technol.*, 58: 277–289.

Akpan, U.G., Hameed, B.H. 2010. The advancements in sol–gel method of doped-TiO₂ photocatalysts. *Appl. Catal A: Gen.*, 375: 1–11.

Azizi, F., Bagheri-Mohagheghi, M.-M. 2013. Transition from anatase to rutile phase in titanium dioxide (TiO₂) nanoparticles synthesized by

complexing sol–gel process: effect of kind of complexing agent and calcinating temperature. *J. Sol-Gel. Sci. Technol.*, 65: 329–335.

Behforooz, M.R., Toujali, S., Haji, S. 2012. Structural changes of Ti films under heat processes and Oxygen flow. *Australian J. Basic Appl. Sci.*, 6(8): 316–319.

Czanderna, A.W., Rao, C.N.R., Honig, J.M. 1958. The anatase-rutile transition. Part 1., Kinetics of the transformation of pure anatase. *Trans. Faraday Soc.*, 54: 1069.

Daniel, L.S., Nagai, H., Aoyama, S., Mochizuki, C., Hara, H., Baba, N., Sato, M. 2012. Percolation threshold for electrical resistivity of Ag-nanoparticle/Titania composite thin films fabricated using molecular precursor method. *J. Mater. Sci.*, 47(8): 3890–3899.

Grabowska, E., Zaleska, A., Sorgues, S., Kunst, M., Etcheberry, A., Colbeau-Justin, C., Remita, H. 2013. Modification of titanium (IV) dioxide with small silver nanoparticles: Application in Photocatalysis. *J. Phys. Chem. C.*, 117(4): 1955–1962.

Guana, H., Wang, X., Guo, Y., Shao, C., Zhang, X., Liu, Y., Louh, R-F. 2013. Controlled synthesis of Ag-coated TiO₂ nanofibers and their enhanced effect in photocatalytic applications. *Appl. Surf. Sci.*, 280: 720–725.

Han, S., Zhang, X., Yu, Q., Lei, L. 2012. Preparation of TiO₂/ITO film electrode by AP-MOCVD for photoelectrocatalytic application. *Sci. China Chem.*, 55(11): 2462–2470.

Hanaor, A.H.D., Sorrell, C.C. 2011. Review of the anatase to rutile phase transformation. *J. Mater. Sci.*, 46: 855–874.

- Hirano, M., Nakahara, N., Ota, K., Tanaike, O., Inagaki, N. 2003. Photoactivity and phase stability of ZrO₂-doped anatase-type TiO₂ directly formed as nanometer-sized particles by hydrolysis under hydrothermal conditions. *J. Solid State Chem.*, 170: 39–49.
- Hou, Y.Q., Zhuang, D.M., Zhang, G., Zhao, M., Wu, M.S. 2003. Influence of annealing temperature on the properties of titanium oxide thin film. *Appl. Surf. Sci.*, 218: 98–106.
- Hu, Y., Tsai, H.L., Huang, C.L. 2003. Phase transformation of precipitated TiO₂ nanoparticles. *Mater. Sci. Eng. A.*, 344: 209–214.
- Huang, C-H., Lin, Y-M., Wang, I-K., Lu, C-M. 2012. Photocatalytic activity and characterization of carbon-modified titania for visible-light-active photodegradation of nitrogen oxides. *Int. J. Photoenergy*, Article ID 548647: 1–13.
- Ishizawa, H., Ogino, M. 1999. Hydrothermal precipitation of hydroxyapatite on anodic titanium oxide films containing Ca and P. *J. Mater. Sci.*, 34: 5893–5898.
- Ji, X., Lou, W., Wang, Q., Ma, J., Xu, H., Bai, Q., Liu, C., Liu, J. 2012. Sol-gel-derived hydroxyapatite-carbon nanotube/titania coatings on titanium substrates. *Int. J. Mol. Sci.*, 13: 5242–5253.
- Jing, Z., Qian, X., Zhaochi, F., Meijun, L., Can, L. 2008. UV Raman spectroscopic study on TiO₂. II. Effect of nanoparticle size on the outer/inner phase transformations. *Angew Chem. Int. Ed.*, 47: 1766–1772.
- Kang, J-G., Sohn, Y. 2011. Interfacial nature of Ag nanoparticles supported on TiO₂ photocatalysts. *J. Mater. Sci.*, 47(2): 824–832.
- Kim, D.J., Hahn, S.H., Oh, S.H., Kim, E.J. 2002. Influence of calcination temperature on structural and optical properties of TiO₂ thin films prepared by sol-gel dip coating. *Mater Lett.*, 57: 355–360.
- Kumar, S.R., Pillai, S.C., Hareesh, U.S., Mukundan, P., Warriar, K.G.K. 2000. Synthesis of thermally stable, high surface area anatase- alumina mixed oxides. *Mater. Lett.*, 43(5–6): 286–290
- Landmann, M., Rauls, E., Schmidt, W.G. 2012. The electronic structure and optical response of rutile, anatase and brookite TiO₂. *J. Phys. Condens. Matter*, 24: 195503–195510.
- Li, G., Boerio-Goates, J., Woodfield, B.F., Li, L. 2004. Evidence of linear lattice expansion and covalency enhancement in rutile TiO₂ nanocrystals. *Appl. Phys. Lett.*, 85: 2059.
- Ma, Q., Qin, TP., Liu, S.J., Weng, L.Q., Dong, W.Y. 2010. Morphology and photocatalysis of mesoporous titania thin films annealed in different atmosphere for degradation of methyl orange. *Appl. Phys. A*, 104(1): 365–373.
- Maldonado-Ho ´dar FJ, Moreno-Castilla C, Rivera-Utrilla J (2000). Synthesis, pore texture and surface acid–base character of TiO₂/carbon composite xerogels and aerogels and their carbonized derivatives. *Appl. Catal. A.*, 203(151): 235–243.
- Meng, Q., Li, X., Liu, L., Cao, B. 2012. High-temperature preparation and electrochemical properties of TiO₂anatase phase-mounted carbon aerogels. *J. Mater. Sci.*, 47: 5926–5932.
- Nagai, H., Mochizuki, C., Hara, H., Takano, I., Sato, M. 2008. Enhanced UV-sensitivity of Vis-responsive anatase

- thin films fabricated by using precursor solutions involving Ti complexes. *Sol. Energ. Mat. Sol. Cell*, 92: 1136–1144.
- Nagai, H., Sato, M. 2012. Heat treatment in molecular precursor method for fabricating metal oxide thin films. *InTech*, Chapt. 5, 103–128.
- Nasser, S.A. 2000. X-ray photoelectron spectroscopy study on the composition and structure of BaTiO₃ thin films deposited on silicon. *Appl. Surf. Sci.*, 157: 14–22.
- Nishide, T., Sato, M., Hara, H. 2000. Crystal structure and optical property of TiO₂ gels and films prepared from Ti-edta complexes as titania precursors. *J. Mater. Sci.*, 35: 465–469.
- Reddy, K.R., Nakata, K., Ochiai, T., Murakami, T., Tryk, D.A., Fujishima, A. 2011. Facile fabrication and photocatalytic application of Ag nanoparticles-TiO₂ nanofiber composites. *J. Nanosci. Nanotechnol.*, 11(4): 3692–3695.
- Shchipunov, Y., Postnova, I. 2009. One-pot biomimetic synthesis of monolithic titania through mineralization of polysaccharide. *Colloid Surf B.*, 74: 172–177.
- Shin, H., Jung, H.S., Hong, K.S., Lee, J.K. 2005. Crystal phase evolution of TiO₂ nanoparticles in aqueous solutions via a freeze-drying method. *J. Solid State Chem.*, 178(15): 324–249.
- Spurr, R.A., Myers, H. 1957. Quantitative analysis of anatase-rutile mixtures with an X-ray diffractometer. *Anal. Chem.*, 29: 760. doi:10.1021/ac60125a006.
- Stamate, M., Lazar, G., Lazar, I. 2008. Anatase-rutile TiO₂ thin films deposited in a D.C. magnetron sputtering system, Rom. *J. Phys.*, 53: 217–221.
- Tian-hua, X., Chen-lu, S., Yong, L., Gao-rong, H. 2006. Band structures of TiO₂ doped with N, C and B. *J. Zhejiang Univ. Sci. B.*, 7(4): 299–303.
- Toda, K., Kawakami, M., Uematsu, K., Sato, M. 2003. Low temperature synthesis of titania and titanates. *Key Eng. Mater.*, 248: 107–110.
- Uekawa, N., Suzuki, M., Ohmiya, T., Mori, F., Wu, Y.J., Kakegawa, K. 2003. Synthesis of rutile and anatase TiO₂ nanoparticles from Ti-peroxy compound aqueous solution with polyols. *J. Mater. Res.*, 18: 797–803
- Yoganarasimhan, S.R., Rao, C.N.R. 1962. Mechanism of crystal structure transformations. Part 3.—Factors affecting the anatase-rutile transformation. *Trans. Faraday Soc.*, 58: 1579–1593.
- Yu, J-G., Yu, H-G., Cheng, B., Zhao, X-J., Yu, J.C., Ho, W-K. 2003. The effect of calcination temperature on the surface microstructure and photocatalytic activity of TiO₂ thin films prepared by liquid phase deposition. *J. Phys. Chem. B.*, 107: 13871–13879.
- Zhang, F-J., Oh, W-C. 2010. Characterization and photonic effect of novel Ag-CNT/TiO₂ composites and their bactericidal activities. *Bull. Korean Chem. Soc.*, 31(7): 1981–1987.
- Zhang, W.F., He, Y.L., Zhang, M.S., Yin, Z., Chen, Q. 2000. Raman scattering study on anatase TiO₂ nanocrystals. *J. Phys. D.*, 33: 912–923.